

Ghost poles and chiral symmetry in πN scattering*

C.A. da Rocha[†]

Department of Physics, Box 351560, University of Washington, Seattle, Washington 98195-1560

G. Krein[‡]

*Instituto de Física Teórica - Universidade Estadual Paulista
Rua Pamplona 145, 01405-900 São Paulo-SP, Brazil*

L. Wilets[§]

*Department of Physics, Box 351560, University of Washington, Seattle, Washington 98195-1560
(May 96)*

We solve the Schwinger-Dyson equation for the nucleon propagator in the vacuum using π , σ , and ω mesons. For bare interaction vertices (Hartree-Fock approximation) we obtain a pair of complex-conjugated poles (ghost poles) and for vertices dressed by phenomenological form-factors these ghosts disappeared. We use these two different approaches to evaluate the scattering lengths and the phase shifts for the πN scattering at threshold. Our results show that only when the form factors are present is possible to obtain a good agreement with the low-energy observables.

I. INTRODUCTION

In recent years a renewed interest in πN scattering is being witnessed in the literature [1,2,3], driven mainly by the necessity of having a relativistic description of the available high energy data, as well as of the data to be generated at CEBAF. Also, the recognition of chiral symmetry as a fundamental symmetry of the strong interactions has motivated a great deal of attention to the role of this symmetry in hadronic processes. The mathematical complexities presented by QCD at low energies require us to use models with effective degrees of freedom as, for instance, the relativistic quantum field model with baryon and meson degrees of freedom, which we adopted in this work. In this approach, to go beyond the perturbative scheme, one must evaluate the nucleon self-energy by solving the Schwinger-Dyson equation (SDE) and obtain a “dressed” nucleon propagator. The simplest first step calculation is to consider “bare” vertex interaction and bare meson propagators, which is known as Hartree-Fock approximation, and use the low-lying mesons in the SDE [4,5]. Using the π , ρ and ω mesons, the main result of this first approach is the appearance of complex poles, or *ghost poles*, in the renormalized nucleon propagator. These ghosts violate basic theorems of quantum field the-

ory and their origin is related to the ultraviolet behavior of the model interactions. The ghosts disappear when form factors that soften the interaction sufficiently in the ultraviolet are used [6]. Since these previous approaches did not consider the role of chiral symmetry, one interesting point is to know how this symmetry can affect the nucleon self-energies and the related observables.

In this work we investigated the πN scattering using a linear realization of chiral symmetry, which is implemented by the linear σ -model lagrangian augmented with the ω meson [7]. The nucleon propagator is obtained by solving the SDE by the iteration method. We use this propagator to evaluate the πN observables at threshold in two different situations: with bare interaction vertices and with vertices dressed by phenomenological formfactors.

II. THE NUCLEON SPECTRAL FUNCTION

In this paper we use the spectral representation of the nucleon propagator and of its inverse. We refer the reader to Refs. [8,9,10] for more details about this approach. The nucleon propagator is defined as

$$G_{\alpha\beta}(x' - x) = -i < 0|T[\psi_\alpha(x')\bar{\psi}_\beta(x)]|0>, \quad (1)$$

where $|0>$ represents the physical vacuum state. The Källen-Lehmann representation for the Fourier transform $G(p)$ of $G(x' - x)$ can be written as

$$G(p) = \int_{-\infty}^{+\infty} d\kappa \frac{A(\kappa)}{p - \kappa + i\epsilon}, \quad (2)$$

where $A(\kappa)$ is the spectral function. It represents the probability that a state of mass $|\kappa|$ is created by ψ or $\bar{\psi}$,

*Contribution presented at the 14th International Conference on Particles and Nuclei (PANIC 96), Williamsburg, VA, 22-28 May 1996.

[†]Fellow from CNPq, Brazilian Agency. Electronic address: carocha@phys.washington.edu

[‡]Electronic address: gkrein@axp.ift.unesp.br

[§]Electronic address: wilets@nuc2.phys.washington.edu

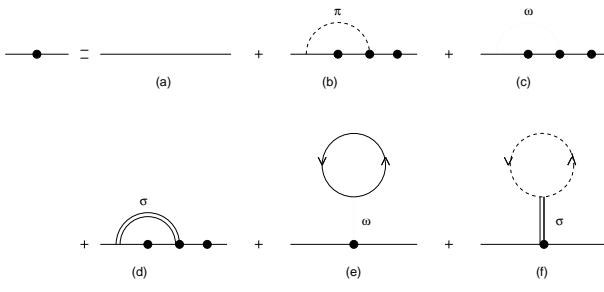


FIG. 1. Diagrammatic representation of SDE. The tadpole diagrams do not contribute because they drop out in the renormalization process.

and as such it must be non-negative. Negative κ corresponds to states with opposite parity to the nucleon. The SDE for the nucleon propagator in momentum space is given by the following expressions

$$G(p) = G^{(0)}(p) + G^{(0)}(p)\Sigma(p)G(p), \quad (3)$$

where

$$\begin{aligned} \Sigma(p) = & -ig_0^2 \int \frac{d^4 q}{(2\pi)^4} \gamma_5 \tau^i D_\pi(q^2) G(p-q) \Gamma_5^i(p-q, p; q) \\ & + ig_0^2 \omega \int \frac{d^4 q}{(2\pi)^4} \gamma_\mu D_\omega^{\mu\nu}(q^2) G(p-q) \Gamma_\nu(p-q, p; q) \\ & + ig_0^2 \int \frac{d^4 q}{(2\pi)^4} D_\sigma(q^2) G(p-q) \Gamma_S(p-q, p; q), \quad (4) \end{aligned}$$

is the nucleon self-energy, shown schematically in Fig. 1.

In Eq. (4), D_π , $D_\omega^{\mu\nu}$, and D_σ are the π , ω , and σ propagators and $\Gamma_5^i(p-q, p; q)$, $\Gamma_\nu(p-q, p; q)$, and $\Gamma_S(p-q, p; q)$ are respectively the pion-nucleon, omega-nucleon, and sigma-nucleon vertex functions. The tadpoles in Fig. 1 do not contribute to the nucleon propagator, since they drop out in the renormalization procedure. The Hartree-Fock (HF) approximation amounts to using the noninteracting meson propagators and bare vertices $\Gamma_5^j(p-q, p; q) = \tau^j \gamma_5$, $\Gamma_\nu(p-q, p; q) = \gamma_\nu$, and $\Gamma_S(p-q, p; q) = 1$ in Eq. (4). In order to regulate the ultraviolet behavior of the interaction and study the role of a ghost-free self-consistent propagator, we consider simplified vertex functions that are written as:

$$\Gamma_5^i(p_1, p_2; q) = \tau^i \gamma_5 F_5(p_1, p_2; q) \quad (5)$$

$$\Gamma^\mu(p_1, p_2; q) = \gamma^\mu F_V(p_1, p_2; q) \quad (6)$$

$$\Gamma_S(p_1, p_2; q) = F_S(p_1, p_2; q), \quad (7)$$

where $F_5(p_1, p_2; q)$, $F_V(p_1, p_2; q)$, and $F_S(p_1, p_2; q)$ are scalar functions. Next we solve the SDE by iteration [6] and we obtain:

$$T_R(\kappa) = \int_{-\infty}^{+\infty} d\kappa' K(\kappa, \kappa') A_R(\kappa'), \quad (8)$$

where $K(\kappa, \kappa')$ is the scattering kernel given by

$$\begin{aligned} K(\kappa, \kappa') = & K_\pi(\kappa, \kappa'; m_\pi^2) \\ & + 2K_\omega(\kappa, \kappa'; m_\omega^2) + K_\sigma(\kappa, \kappa'; m_\sigma^2); \quad (9) \end{aligned}$$

with $K_\pi(\kappa, \kappa'; m_\pi^2)$, $K_\omega(\kappa, \kappa'; m_\omega^2)$, and $K_\sigma(\kappa, \kappa'; m_\sigma^2)$ being respectively the π , ω , and σ contributions, given by

$$\begin{aligned} K_\pi(\kappa, \kappa'; m_\pi^2) = & F_5(\kappa, \kappa'; m_\pi) 3 \left(\frac{g}{4\pi} \right)^2 \frac{1}{2|\kappa|^3} \\ & \times [(\kappa - \kappa')^2 - m_\pi^2] \theta(\kappa^2 - (|\kappa'| + m_\pi)^2) \\ & \times [\kappa^4 - 2\kappa^2(\kappa'^2 + m_\pi^2) + (\kappa'^2 - m_\pi^2)^2]^{1/2}, \quad (10) \end{aligned}$$

$$\begin{aligned} K_\omega(\kappa, \kappa'; m_\omega^2) = & F_V(\kappa, \kappa'; m_\omega) \left(\frac{g_\omega}{4\pi} \right)^2 \frac{1}{2|\kappa|^3} \\ & \times [(\kappa - \kappa')^2 - 2\kappa\kappa' - m_\omega^2] \theta(\kappa^2 - (|\kappa'| + m_\omega)^2) \\ & \times [\kappa^4 - 2\kappa^2(\kappa'^2 + m_\omega^2) + (\kappa'^2 - m_\omega^2)^2]^{1/2}, \quad (11) \end{aligned}$$

and

$$\begin{aligned} K_\sigma(\kappa, \kappa'; m_\sigma^2) = & F_S(\kappa, \kappa'; m_\sigma) \left(\frac{g}{4\pi} \right)^2 \frac{1}{2|\kappa|^3} \\ & \times [(\kappa + \kappa')^2 - m_\sigma^2] \theta(\kappa^2 - (|\kappa'| + m_\sigma)^2) \\ & \times [\kappa^4 - 2\kappa^2(\kappa'^2 + m_\sigma^2) + (\kappa'^2 - m_\sigma^2)^2]^{1/2}. \quad (12) \end{aligned}$$

In the above equations, g and g_ω are the renormalized coupling constants, defined as $g = Z_2 g_0$ and $g_\omega = Z_2 g_{0\omega}$, where Z_2 is the renormalization constant [6]. The spectral functions $A_R(\kappa)$ and $T_R(\kappa)$ are related by

$$A_R(\kappa) = \delta(\kappa - M) + |\tilde{G}_R^{-1}(\kappa(1 + i\epsilon))|^{-2} T_R(\kappa) \quad (13)$$

$$\equiv \delta(\kappa - M) + \bar{A}_R(\kappa). \quad (14)$$

where

$$\begin{aligned} \tilde{G}_R^{-1}(z) = & (z - M) \times \\ & \left[1 - (z - M) \int_{-\infty}^{+\infty} d\kappa \frac{T_R(\kappa)}{(\kappa - M)^2 (z - \kappa)} \right]. \quad (15) \end{aligned}$$

Initially, we consider bare vertices: $F_5(p_1, p_2, q) = F_V(p_1, p_2, q) = F_S(p_1, p_2, q) = 1$, and study the convergence properties of the SDE for the nucleon self-energy. We use the following values for the coupling constants:

$$\frac{g_\pi^2}{4\pi} = \frac{g_\sigma^2}{4\pi} \equiv \frac{g^2}{4\pi} = 14.6 \quad \text{and} \quad \frac{g_\omega^2}{4\pi} = 6.36, \quad (16)$$

where we wrote explicitly that the value of the sigma-nucleon coupling constant is equal to the pion-nucleon

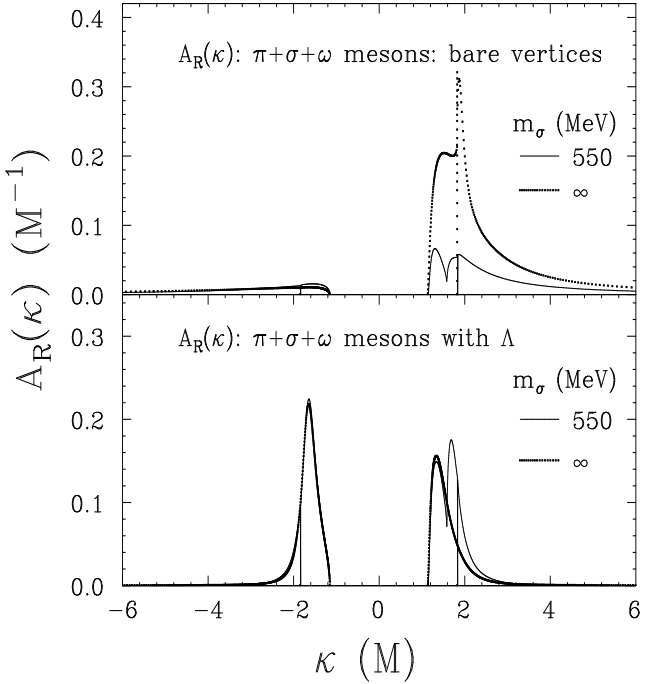


FIG. 2. *Top*: plot of $A_R(\kappa)$ as a function of κ for nucleon self-energy due to $\pi+\sigma+\omega$ mesons with *bare* nucleon vertices. *Bottom*: the same study for the same system but with vertices dressed by form factors.

one, as required by the linear realization of chiral symmetry.

We first solved the SDE for bare interaction vertices and we observed that the introduction of the chiral partner of the pion *does not remove* the ghost poles. As the mass of the σ meson remains a point of debate, we varied m_σ over a wide range. The solutions of SDE converge quickly in the studied range, $500 \leq m_\sigma \leq 1500$ MeV. The converged spectral functions $A_R(\kappa)$ are shown in Fig. 2. We used the following values for the meson masses:

$$m_\pi = 138.03 \text{ MeV} , \quad (17)$$

$$m_\omega = 783 \text{ MeV} , \quad (18)$$

$$m_\sigma = 550, 770, 980 \text{ MeV and } m_\sigma \rightarrow \infty . \quad (19)$$

The reason for using this particular set of σ masses is the following: $m_\sigma = 550$ MeV is the value commonly used in the One Boson Exchange Potentials (OBEP) [12]; $m_\sigma = 770$ MeV is the value used by Serot and Walecka [13] in the calculations of nuclear matter properties using the chiral linear sigma model; $m_\sigma = 980$ MeV is the first scalar meson in the mesons table, f_0 , and the limit $m_\sigma \rightarrow \infty$ supplies the connection between the linear realization of chiral symmetry and the minimal chiral model of the non-linear realization of chiral symmetry in πN system [14].

Fig. 2-top presents the nucleon dressed by the $\pi+\sigma+\omega$

mesons, for $m_\sigma = 550$ MeV and $m_\sigma \rightarrow \infty$. We note that $A_R(\kappa)$ for positive κ is much larger than for negative κ , it increases as the σ mass increases, and becomes equal to the $\pi+\omega$ case in the limit $m_\sigma \rightarrow \infty$, since the σ meson does not contribute to $A_R(\kappa)$ in this limit.

Next we consider vertex form factors. In principle one can use the corresponding Sudakov form factors, as in Ref. [6]. However, since the Sudakov form factor is known exactly in the ultraviolet only, one has to interpolate it in some way down to the infrared or simply parametrize its infrared behavior. However, since for our purposes here of killing the ghosts the infrared behavior is not relevant, we prefer to simplify matters and use parametrized form factors. For general off-shell legs, we use the factorized form of Pearce and Jennings [1]; for a vertex with four-momenta $p_\alpha, p_\beta, p_\gamma$, the form factor is

$$F_{\alpha\beta\gamma} = F_\alpha(p_\alpha^2) F_\beta(p_\beta^2) F_\gamma(p_\gamma^2) . \quad (20)$$

For mesons we adopt the expressions by Gross, Van Orden and Holinde [15]

$$F_m(q^2) = \left[\frac{1 + (1 - \mu_m^2/\Lambda_m^2)^2}{1 + (1 - q^2/\Lambda_m^2)^2} \right]^2 \quad (21)$$

where Λ_m is the meson cutoff mass. For the nucleon legs we adopt the expressions by Gross and Surya [2]

$$F_B(p^2) = \frac{(\Lambda_B^2 - m_B^2)^2}{(\Lambda_B^2 - m_B^2)^2 + (m_B^2 - p^2)^2} \quad (22)$$

where Λ_B is the nucleon cutoff mass. Both meson and nucleon form factors have the correct on-shell limit, equal to unity.

At this point it is perhaps convenient to call attention that we use form factors for regulating the ultraviolet with the only aim of studying the role of a ghost-free propagator in πN scattering. In principle, the form factors are calculable within the model by means of vertex corrections. In particular, such vertex corrections must satisfy Ward-Takahashi identities that follow from chiral symmetry, and of course our form factors F_m and F_B , Eq. (21), do not satisfy such identities. This interesting subject is intended to be pursued in a future work.

The cutoff values Λ_B and Λ_m are constrained to kill the ghost poles and give the best fit to the scattering lengths. Fig. 2-bottom presents the case $\pi + \sigma + \omega$, with form factors at each vertex. We use $\Lambda_B = 1330$ MeV. The shape of $A_R(\kappa)$ depends strongly on the σ mass for $\kappa > 0$ only. One sees that the second peak is mainly due to the σ meson, it decreases as the σ mass increases and disappears in the limit $m_\sigma \rightarrow \infty$. The interesting effect due to the form factors is that the spectral function for $\kappa < 0$ becomes very large as compared to the case of bare vertices. This will have serious consequences for the observables of πN scattering.

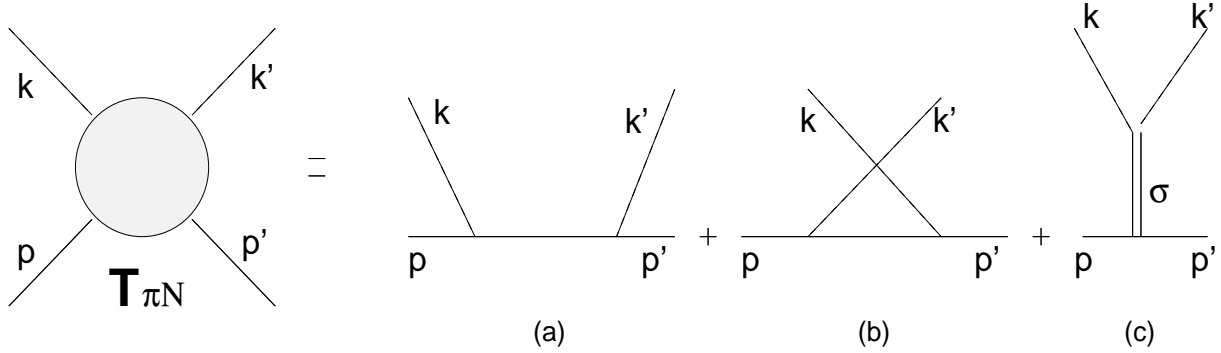


FIG. 3. (a),(b) Order g^2 contributions involving only pions and nucleons, where the πNN coupling is pseudoscalar. (c) Scalar meson contribution.

III. πN SCATTERING

In Born approximation, when using pions and nucleons only, the lowest order contribution is the sum of just two graphs, as shown in Figs. 3(a,b). It is well known that the first two contributions give bad results for isoscalar observables when the πNN coupling is pseudoscalar.

As we introduce the $\pi\pi\sigma$ and σNN couplings by means of the chiral symmetry the diagram of Fig. 3(c) appears, which inclusion led to an almost perfect fit to the value of the isospin-even amplitude $A^{(+)}$ at threshold. This is one of the classical examples of the importance of chiral symmetry in hadronic interactions.

The πN amplitude $T_{\pi N}$ can be parameterized as [16]

$$T_{\pi N} = \bar{u}(\mathbf{p}') \left\{ \left[A^+ + \frac{1}{2} (\not{k} + \not{k}') B^+ \right] \delta_{ab} + \left[A^- + \frac{1}{2} (\not{k} + \not{k}') B^- \right] i \epsilon_{bac} \tau_c \right\} u(\mathbf{p}), \quad (23)$$

The contribution of the non-delta part of the spectral function, defined in Eq. (14), to the functions A^\pm, B^\pm is given by:

$$A^\pm(s, t, u) = g^2 \int_{-\infty}^{\infty} d\kappa \bar{A}(\kappa) (\kappa - M) \left[\frac{1}{s - \kappa^2} \pm \frac{1}{u - \kappa^2} \right] \quad (24)$$

$$B^\pm(s, t, u) = g^2 \int_{-\infty}^{\infty} d\kappa \bar{A}(\kappa) \left[-\frac{1}{s - \kappa^2} \pm \frac{1}{u - \kappa^2} \right] \quad (25)$$

The total contribution for A^\pm and B^\pm is the sum of three parts coming from: (a) the delta function part of $A(\kappa)$ (nucleon pole term), (b) the self-energy given by Eqs. (24-25), and in the case of bare vertices (c) the ghost poles. The contribution from the ghosts poles is given by:

$$A_g^\pm(s, t, u) = g^2 \sum_c A_c (\kappa_c - M) \left[\frac{1}{s - \kappa_c^2} \pm \frac{1}{u - \kappa_c^2} \right] \quad (26)$$

$$B_g^\pm(s, t, u) = g^2 \sum_c A_c \left[-\frac{1}{s - \kappa_c^2} \pm \frac{1}{u - \kappa_c^2} \right], \quad (27)$$

where κ_c is the pole position and A_c is the residue and the sum is over (κ_c, A_c) and its complex conjugate (κ_c^*, A_c^*) .

Tab. I shows the results for A^+ and the scattering lengths a^\pm for two cases: $m_\pi = 138.03$ MeV and the chiral limit $m_\pi = 0$. The low-energy theorems impose in the second case that $A^+ = 1$ (in g^2/M units) and $a^\pm = 0$. All results are obtained with no form factors in either the Schwinger-Dyson equation nor in the scattering amplitudes.

The results for the scattering lengths should be compared with the experimental values given by [17]

$$a^+ = -(0.021 \pm 0.021) \text{ fm}$$

$$a^- = 0.139 \begin{cases} +0.004 & \text{fm} \\ -0.010 & \text{fm} \end{cases} \quad (28)$$

TABLE I. Results for observables using dressed nucleon propagators: (a) $m_\pi = 138.08$ MeV and (b) the chiral limit $m_\pi \rightarrow 0$. No form factors are used.

Contribution	(a) $m_\pi = 138.08$ MeV			(b) $m_\pi = 0$		
	A^+ (g^2/M)	a^+ (fm)	a^- (fm)	A^+ (g^2/M)	a^+ (fm)	a^- (fm)
1) $\pi + \sigma(550) + \omega$: $A_R(\kappa)$	0.0197	0.0773	0.1108	0.0202	0.0619	0
2) $\pi + \sigma(550) + \omega$: ghosts	-0.5894	-1.9462	1.8702	-0.7717	-2.3679	0
3) $\pi + \sigma(550) + \omega$: Tree diagrs.	0.9370	-0.1830	0.1977	1.0	0	0
Sum (A): 1 + 2 + 3	0.3673	-2.0520	2.1790	0.2484	-2.3606	0
4) $\pi + \sigma(\infty) + \omega$: $A_R(\kappa)$	-0.1659	-0.3935	0.0891	-0.2067	-0.6342	0
5) $\pi + \sigma(\infty) + \omega$: ghosts	0.9906	2.6735	-0.0821	1.0839	0.9314	0
6) $\pi + \sigma(\infty) + \omega$: Tree diagrs.	1.0	-0.01453	0.1977	1.0	0	0
Sum (B): 10 + 11 + 12	1.8247	2.2654	0.2074	1.8772	2.6917	0

TABLE II. Same as in TABLE I, but using form factors.

Contribution	A^+ g^2/M	$m_\pi \cdot B^+$ g^2/M	A^- g^2/M	$m_\pi \cdot B^-$ g^2/M	a^+ (fm)	a^- (fm)
1) $\pi + \sigma(550) + \omega$: $A_R(\kappa)$	0.3744	0.0249	0.1335	0.0644	1.06820	0.5292
2) $\pi + \sigma(550) + \omega$: Tree diagrs.	0.3986	-0.8335	0	0.0613	-1.16336	0.1639
Sum (A): 1 + 2	0.7730	-0.8084	0.1335	0.1267	-0.09516	0.6931
3) $\pi + \sigma(\infty) + \omega$: $A_R(\kappa)$	0.3815	0.0246	0.1329	0.0601	1.08640	0.5163
4) $\pi + \sigma(\infty) + \omega$: Tree diagrs.	0.4211	-0.8335	0	0.0613	-1.10326	0.1639
Sum (B): 7 + 8	0.8026	-0.8089	0.1329	0.1214	-0.01686	0.6802

and with the predictions of the low-energy theorems. Inspecting Tab. I, we see that the observable a^+ are very far from the experimental result and the observables in the chiral limit are poor described.

In order to improve the description of the data, we dressed the interaction vertices with the formfactors. We fix the cutoff values by fixing the right values of the low-energy theorems. Tab. II presents the results for the observables for $m_\pi = 138.03$ MeV.

Observable A^+ receives contributions mainly from (a) the σ -exchange, Fig. 3(c), which depends directly on Λ_m , and (b) from the nucleon self-energy $\bar{A}_R(\kappa)$, which is weakly dependent on Λ_B and is almost independent from the σ mass. The results show that σ exchange and the self-energy contribution $\bar{A}_R(\kappa)$ contribute approximately 50% each. The results for a^+ depend on the sum of A^+ and B^+ . Observable B^+ receives contributions from the nucleon Born part, Fig. 3(a),(b), and from the spectral function $\bar{A}_R(\kappa)$. The contribution from the spectral function is almost constant and very small. The contribution from nucleon pole term depends very weakly on Λ_B . For $\Lambda_B = 1.2 \rightarrow 1.4$ GeV, we obtain $m_\pi \cdot B^+ = -0.78 \rightarrow -0.86 g^2/M$. Therefore the way to get the almost zero result for a^+ is decreasing the A^+ contribution from 1 (without form factor) to 0.8 g^2/M , adjusting Λ_m , since $m_\pi \cdot B^+ \approx -0.8$.

Observable a^- is not well adjusted due to the huge contribution from $\bar{A}_R(\kappa)$, being almost 75% of the final result. This huge contribution comes from negative κ part of the spectral function. We checked this point by doing $\bar{A}_R(\kappa) = 0$ for $\kappa < 0$ by hand and get a result 5 times smaller for a^- . As discussed previously, the negative κ enhancement is an effect due to the form factors.

Now we show the phase shifts results. The total amplitude for πN scattering may be decomposed into the isospin $\frac{3}{2}$ and $\frac{1}{2}$ channels. The isospin $\frac{3}{2}$ and $\frac{1}{2}$ amplitudes are related to the symmetric and antisymmetric amplitudes by

$$\begin{aligned} O^{(3/2)} &= O^{(+)} - O^{(-)}, \\ O^{(1/2)} &= O^{(+)} + 2O^{(-)}. \end{aligned} \quad (29)$$

where O can be A or B . Therefore, the T matrix can be decomposed into good isospin and total angular momentum channels to reveal the existence of any resonances.

The optical theorem identifies the total cross section with the imaginary part of the scattering amplitude. We unitarize the amplitude following the method of Olsson and Osypowski [17]. Fig. 4 presents the results for the phase shifts for $\ell = 0$ waves. The agreement near threshold is very good, and the model fails for higher energies. The other phase-shifts show the same trend: they are well described near threshold, but as energy increases the agreement with data becomes poor.

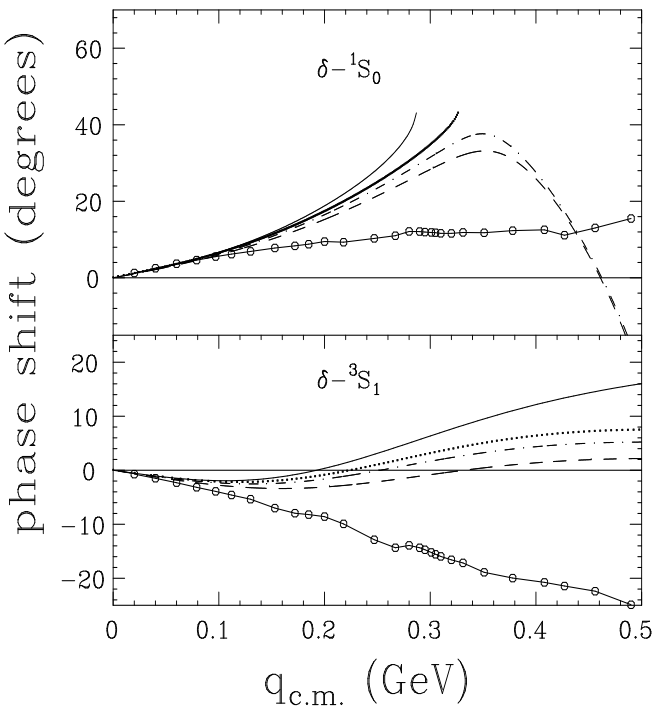


FIG. 4. Phase shifts for $\ell = 0$ waves. The curves represent the choices for the σ -meson mass: 550 MeV (dashed), 770 MeV (dot-dashed), 980 MeV (dotted), and $m_\sigma \rightarrow \infty$ (solid curve). Data are from [18].

IV. CONCLUSIONS

In this contribution we obtained a “dressed” nucleon propagator by solving the SDE with π , σ , and ω mesons. The interaction vertices were extracted from the linear- σ model augmented with the ω meson and we considered two cases: bare and “dressed” vertices, where the dressing is made by phenomenological form factors. The solution of the SDE for bare vertices contains a pair of ghost poles. The sum of ghosts plus σ -meson contributions exceeds by a large amount the experimental values of the a^+ scattering lengths at threshold, spoiling the well-known good agreement of the linear σ -model for the bare nucleon propagator. The next natural step is to go beyond the Hartree-Fock approximation, in order to eliminate the ghosts. If the ghosts are killed by softening the ultraviolet by means of form factors it is possible to obtain qualitative agreement with experimental data of observables at low energies. Another lesson from our study is that the nucleon spectral function $\bar{A}(\kappa)$ for negative κ is strongly enhanced by the form factors and this affects some of the observables. In particular, the negative κ enhancement increases the isospin antisymmetric scattering length a^- . One possible solution for this problem is (a) the inclusion of other resonances like ρ and Δ in the tree diagrams and (b) to include the vertices $\sigma\pi\pi$

and $\rho\pi\pi$ in the Schwinger-Dyson equation. This is highly non-trivial because one has to solve a set of coupled integral equation where the integral is now bidimensional. We intend to tackle this point in a near future publication.

ACKNOWLEDGMENTS

We thank Prof. M. Robilotta and Prof. T. Cohen for the helpful conversations about πN scattering and chiral symmetry. This work was partially supported by U.S. Department of Energy. The work of C.A. da Rocha was supported by CNPq Brazilian Agency.

- [1] B.C. Pearce and B.K. Jennings, Nucl. Phys. **A528**, 655 (1991).
- [2] F. Gross and Y. Surya, Phys. Rev. C **47**, 703 (1993).
- [3] P.F.A. Goudsmit, H.J. Leisi, and E. Matsinos, Phys. Lett. B **299**, 6 (1993).
- [4] W.D. Brown, R.D. Puff, and L. Wilets, Phys. Rev. C **2**, 331 (1970).
- [5] L. Wilets, in *Mesons in Nuclei*, (M. Rho and D. Wilkinson eds., North-Holland, Amsterdam, 1979).
- [6] G. Krein, M. Nielsen, R.D. Puff, and L. Wilets, Phys. Rev. C, **47** 2485 (1993); M.E. Bracco, A. Eiras, G. Krein, and L. Wilets, Phys. Rev. C **49**, 1299 (1994).
- [7] B.J. Lee, *Chiral Dynamics*, (Gordon and Breach, New York 1972).
- [8] S.S. Schweber, *An Introduction to Relativistic Quantum Field Theory*, (Harper & Row, Publ., New York, 1962).
- [9] P. Roman, *Introduction to Quantum Field Theory*, (John Wiley & Sons, Inc., New York, 1969).
- [10] N.N. Bogolubov, A.A. Logunov, and I.T. Todorov, *Axiomatic Quantum Field Theory*, (Benjamin, Reading MA, 1975, pp. 269-270, 330ff, Appendix F).
- [11] V.G.J. Stoks, R.A.M. Klomp, M.C.M. Rentmeester, and J.J. de Swart, Phys. Rev. C **48**, 792 (1993).
- [12] R. Machleidt, K. Holinde, and Ch. Elster, Phys. Rep. **149**, 1 (1987).
- [13] B.D. Serot and J.D. Walecka, *Adv. in Nucl. Phys.*, Vol. **16**, (J.W. Negele and E. Vogt eds., Plenum Press, New York, 1986).
- [14] C.A. da Rocha and M.R. Robilotta, Phys. Rev. C, **49**, 1818 (1994); **52**, 531 (1995).
- [15] F. Gross, J.W. Van Orden, and K. Holinde, Phys. Rev. **45**, 2094 (1992).
- [16] W.T. Nutt and L. Wilets, Phys. Rev. D **11**, 110 (1975).
- [17] M.G. Olsson and E.T. Osypowski, Nucl. Phys. **B101**, 136 (1975).
- [18] G. Höhler, Pion-nucleon scattering, in *Landolt - Börnstein*, Vol. **I/9B-2**, (H. Schopper, ed., Springer Verlag, Heidelberg, 1983).